Aging of Insulated Metal Substrate Printed Circuit Boards Under High-Frequency Voltage Stress

Lagerweij, Gijs Willem; Niasar, Mohamad Ghaffarian

DOI
10.1109/TDEI.2025.3562177

Publication date
2025

Document Version
Final published version

Published in
IEEE Transactions on Dielectrics and Electrical Insulation

Aging of Insulated Metal Substrate Printed Circuit Boards Under High-Frequency Voltage Stress

Gijs Willem Lagerweij and Mohamad Ghaffarian Niasar, *Member, IEEE*

***Abstract*— High-end power conversion applications increasingly use insulated metal substrate (IMS) printed circuit boards (PCBs) with very thin dielectrics to improve thermal performance. To ensure the reliability of these PCBs when exposed to high-frequency voltages, the breakdown and aging mechanisms of the PCB laminates under high-frequency voltage stress must be understood. This article investigates the breakdown and lifetime of these laminates using two high-frequency test sources for sinusoidal and square-wave voltages in the typical frequency range of 25–100 kHz and a test voltage up to 8 kV, which is a significant increase compared with the existing literature. Diagnostic tests, such as partial discharge (PD) measurement and dielectric frequency response analysis, are performed to analyze the high-frequency aging mechanisms further. Despite the rapid degradation of the insulation system under high-frequency voltage stresses, the results show that the IMS PCB laminates are quite robust, with high breakdown fields. The lifetime of the PCB laminates is found to vary approximately with the inverse of the frequency. Surface degradation due to the high inhomogeneous fields at the edges of the conducting planes is identified as one of the main lifetime risks. This is similar to more conventional PCB constructions. Diagnostic tests suggest that the accelerated degradation is due to highly localized PD activity and electrical treeing.**

***Index Terms*— Breakdown testing, high-frequency stress, insulated metal substrate (IMS), printed circuit board (PCB).**

I. Introduction

With the increasing demand for power converters with high power density, the need for improved cooling solutions arises. An overview of the most common cooling solutions is given in Fig. 1. In recent years, the insulated metal substrate (IMS) printed circuit board (PCB) has become a low-cost, high-performance cooling solution for high-end power converters based on silicon carbide (SiC) semiconductor devices [1].

Received 16 December 2024; revised 12 March 2025; accepted 14 April 2025. Date of publication 18 April 2025; date of current version 19 December 2025. This work was supported by the High Voltage Technology Group of Delft University of Technology and Prodrive Technologies. *(Corresponding author: Gijs Willem Lagerweij.)*

Gijs Willem Lagerweij is with Prodrive Technologies B.V., 5692 EM Eindhoven, The Netherlands (e-mail: gijs.lagerweij@prodrive-technologies.com).

Mohamad Ghaffarian Niasar is with the High Voltage Technologies Research Group, Delft University of Technology, 2628 CD Delft, The Netherlands.

Digital Object Identifier 10.1109/TDEI.2025.3562177

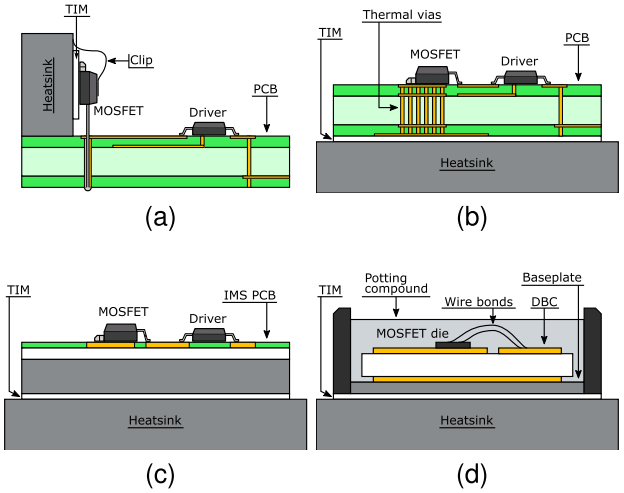

Fig. 1. Comparison of semiconductor cooling solutions: (a) heatsink-mounted devices, (b) surface-mount devices on an FR4 PCB, (c) surface-mount devices on an IMS PCB, and (d) bare dies in a power module. The thermal interface material (TIM) in (a) and (c) also functions as an isolation barrier to the heatsink.

Initially used in power conversion for the telecommunications industry and high-power LED lighting, IMS PCBs are now finding new applications in power electronic converters. However, this shift in application has led to increased electric field stress on the dielectric layer. The insulation material, typically a thin epoxy laminate/prepreg, is exposed to high-voltage ($\geq$1 kV) high-frequency voltage waveforms.

Ample literature is available on breakdown and aging tests performed on PCBs constructed from various materials; see, e.g., [2], [3], [4], [5], [6]. However, the majority of studies focus on surface degradation phenomena on glass-fiber reinforced PCB laminates (like FR4) in a limited frequency range, typically below 25 kHz. Therefore, this article aims to characterize the dielectric degradation and electrical breakdown specifically in IMS PCBs under high-frequency voltage stress up to 100 kHz. The goal is to provide practical insights and mitigate potential lifetime risks in these new power electronics applications.

A. IMS PCB Stackup

Metal-core PCBs consist of an aluminum or copper baseplate, a thin dielectric layer (50–300 μm), and a layer of

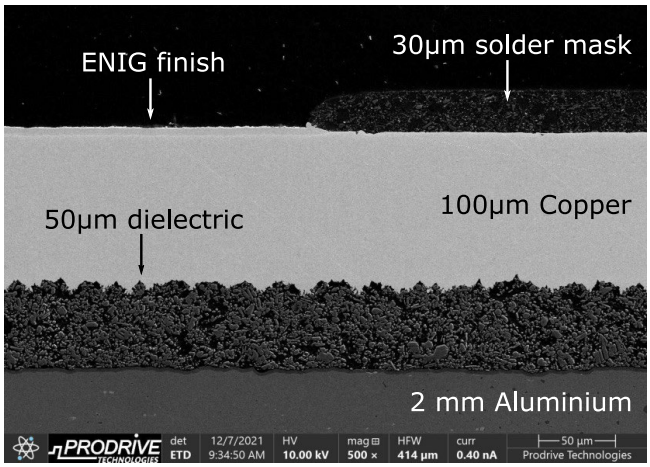

Fig. 2. SEM micrograph of an IMS PCB with 50-µm alumina-filled epoxy dielectric, 3-oz copper, and a 2-mm aluminum base. Image courtesy of Prodrive Technologies.

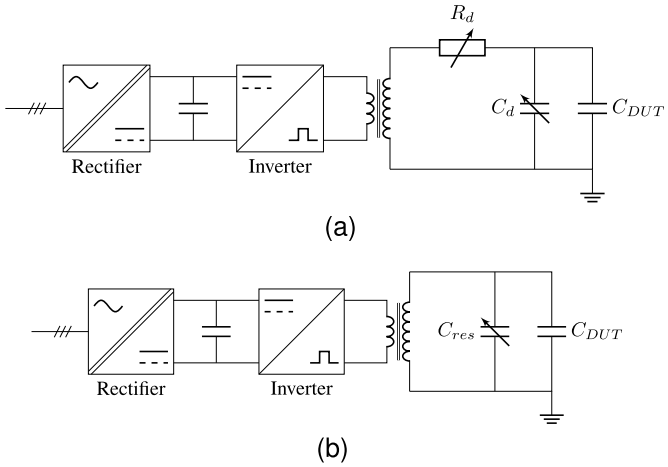

Fig. 3. HV test generators for (a) square-wave voltage and (b) sinusoidal voltage. The device under test is modeled as a capacitor C_{DUT}.

etched copper with or without a solder mask. Typically, the insulating layer comprises an epoxy resin and dense inorganic fillers, which significantly improve the thermal, mechanical, and electrical properties of the dielectric [7], [8]. The most common microfillers are alumina (Al_2O_3) and silica (SiO_2), which improve the thermal conductivity from 0.3 W/(m K) for neat epoxy to 1–4 W/(m K). Nanofillers have been shown to significantly improve partial discharge (PD) resistance, space charge characteristics, and dielectric strength due to an increased deep trap density. Microfillers promote shallow traps and tend to have the opposite effect on these properties [9], [10], [11].

In Fig. 2, a cross section of an IMS PCB with alumina microfilled dielectric (type Ventec VT-4B3) is presented, showing the layers discussed above. Observe that the copper surface has a certain roughness, which allows for an excellent mechanical bond between the copper and the dielectric. This improves mechanical robustness and thermal performance.

B. High-Frequency Aging

The aging of insulation materials such as polyimide, epoxy resin, and oil-paper insulation under repetitive pulsed voltages has been researched in the context of electrical machines and solid-state transformers [12], [13]. In general, the factors negatively influencing lifetime are, in order of importance: 1) voltage/electric field; 2) frequency; and 3) rise time. In addition, there can be environmental influences such as temperature, humidity, and pressure. The inverse power law, which is typically used to calculate electrical lifetime under dc or ac (50/60 Hz) voltage stresses, has been reformulated by Cavallini et al. [14] to include the effect of frequency and rise time by considering not just the rms voltage but also the peak voltage and the harmonic components of the waveform, each with its own inverse power contribution to lifetime.

The most commonly cited reason for the degradation of insulation under high-frequency voltages is PD activity, which may be exacerbated by increased dielectric heating and accumulation of space charge at the electrodes (field emission) and defects (injection by PDs) [15], [16].

C. Outline

In this article, high-voltage tests are performed on representative IMS PCB samples using high-frequency square-wave and sinusoidal voltage waveforms. First, the HV generators and test setup are introduced. Second, the dielectric properties of the samples are measured and discussed. Finally, the samples are tested following a comprehensive approach, including ramp breakdown tests under various conditions, long-duration tests to derive the voltage–life curve at several frequencies, and PD measurements.

II. Test Setup

Considering that the final applications of these PCBs will be in power conversion equipment, tests should be performed in the same frequency range and ideally with representative square-wave voltages. Two HV generators have been designed to replicate the normally occurring stresses.

A. Square-Wave Generator

First, a square-wave generator was designed and qualified [1], [17] for 25–100 kHz and voltages up to 8 kV. An HF transformer based on amorphous magnetic cores is used to amplify a low-voltage square wave, as shown in Fig. 3(a). The transformer is driven by a SiC MOSFET full-bridge with a maximum bus voltage of 400 V. The resulting square-wave voltage has a minimum rise time of 750 ns with less than 5% overshoot. These parameters can be tuned using the damping resistor R_d and capacitor C_d, which is discussed in detail in [17].

B. Sine-Wave Generator

To generate high-frequency sinusoidal voltages, a resonant transformer is used [Fig. 3(b)] following the design presented in [1] and [18]. The test frequency is determined by the leakage inductance of the transformer and its load capacitance, consisting of the DUT and a variable parallel-plate capacitor C_{res}. Using this setup, sinusoidal waveforms are obtained with peak voltages up to 20 kV at frequencies up to 100 kHz. The waveforms are presented in [18].

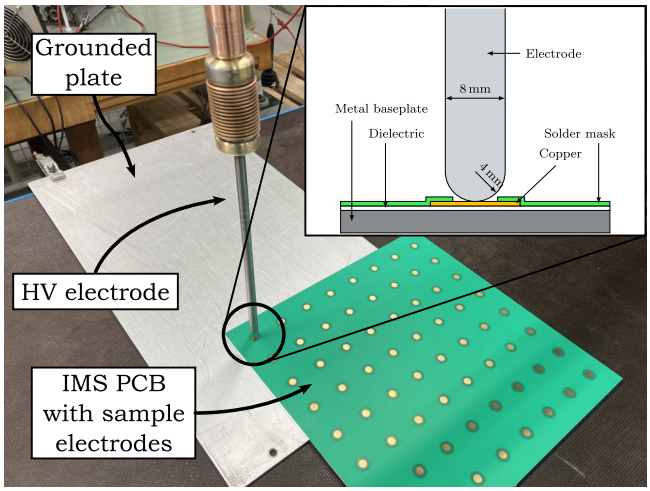

Fig. 4. Sample PCB in test setup with spring-pressurized stainless-steel rod electrode and grounded plate.

C. PCB Samples

PCBs are designed with a grid of circular electrodes of 10-, 20-, and 30-mm diameter and various dielectric thicknesses. Breakdown and electrical aging tests are performed on these samples to characterize their withstand capability and degradation under high-frequency electric stress. To prevent flashover, the clearance between electrodes and board edge is >1.5 cm and tests are performed under oil.

D. Electrode Arrangement

The high voltage is supplied to the copper electrode through a small stainless-steel rod suspended on a 100-kV insulator, as illustrated in Fig. 4. The contact point of the rod is hemispherical, but this has no significant effect on the field distribution, which is dominated by the edge effects of the etched copper planes. The aluminum substrate is grounded by placing the PCB on a grounded metal plate.

III. Dielectric Characterization

Because the dielectric losses appear to play an important role in the degradation mechanisms under high-frequency pulsed stresses, it is necessary to characterize the dielectric spectrum of the insulation material over frequency and temperature. The frequency components of interest are the fundamental and harmonics of the switching frequency. Considering that the practical switching frequency on IMS PCBs is ≤100 kHz, dielectric spectroscopy is performed up to 1 MHz. Dielectric response measurements are performed with a Novocontrol Alpha dielectric spectrometer with a ZGS active sample cell and Quatro Cryosystem for highly accurate temperature control [1].

The dielectric spectrum shown in Fig. 5 exhibits α-relaxation (low-frequency peak due to main chain motion), β-relaxation (high-frequency peak due to polar group motion, e.g., OH and NH groups), and Maxwell–Wagner–Sillars or interfacial polarization due to the microcomposite nature of the dielectric. These polarization and relaxation processes are thermally activated, causing the spectrum to shift toward higher frequencies following the Arrhenius equation as temperature increases [19]. The dielectric losses increase by orders of magnitude as the temperature approaches the glass transition temperature T_g = 130 °C due to the increased mobility of the main polymer chain.

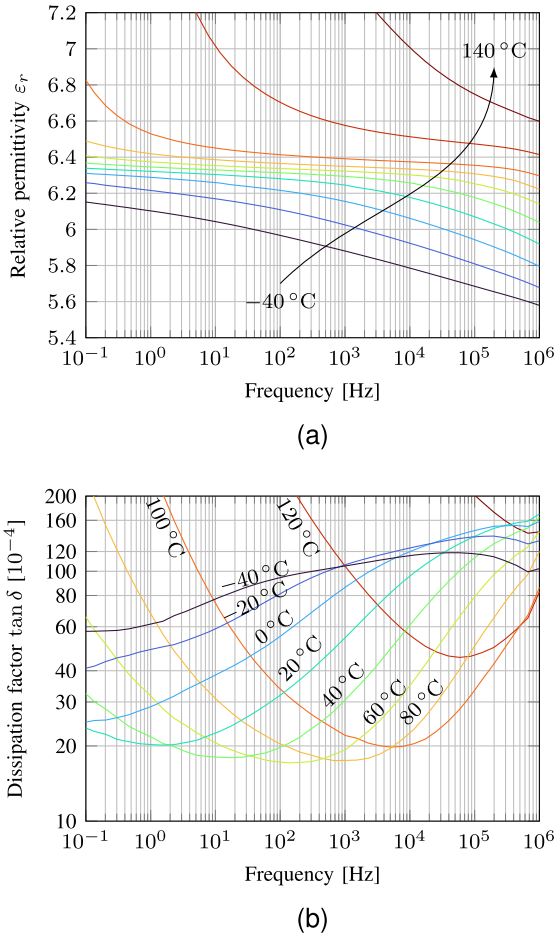

Fig. 5. Dielectric spectrum measured on the 50-μm insulation sample (epoxy with Al_2O_3 microfiller) for temperatures from −40 °C to 140 °C in 20 °C steps. (a) Relative permittivity ε_r. (b) Dissipation factor tanδ.

IV. Ramp Breakdown Tests

Ramp breakdown tests are performed to characterize the material's dielectric strength at various frequencies. Ramp tests are preferred over static tests because they are much faster, and the results have a smaller variance. All the tests are performed with a ramp of 500 V/s to ensure that breakdown occurs between 10 and 20 s of testing. Furthermore, tests were performed under standard laboratory conditions, with an ambient temperature between 17 °C and 21 °C.

A. Weibull Analysis

The breakdown data are fit to a Weibull distribution using maximum likelihood estimation (MLE). If the fit is good, the data will form a straight line on the Weibull plot which has breakdown strength U_{bd} on the x-axis, and the cumulative distribution function (cdf) $F(U)$ on the y-axis. The cdf for

a generic variable x is given by the following equation:

$$F(x) = 1 - \exp\left[-\left(\frac{x}{\eta}\right)^{\beta}\right] \quad (1)$$

where η is the scale parameter with units of x, and β is the unitless shape parameter.

B. Sample Preparation

PCB samples with circular copper electrodes (diameter between 1 and 3 cm), 3-oz copper and 2-mm aluminum baseplate are used for testing. Each PCB houses a grid of 8 × 8 electrodes to save space and cost. The PCBs are preconditioned according to the ASTM D618-B standard for testing dielectric materials (condition 48/50 + Des).

The electrodes have a nearly perfect bond to the dielectric because the copper is evaporated onto it, as shown previously in Fig. 2. However, the sharp edges of the copper electrode, caused by the etching process, result in an inhomogeneous field distribution (see the discussion in Section VII). For this reason, the breakdown strength will be recorded as the voltage U_{bd} instead of the field strength.

C. Challenges

Another effect of the highly inhomogeneous field at the edges of the electrodes is that surface discharges and flashover may occur to neighboring electrodes. Measurements have shown that flashover can occur before the dielectric is punctured. The breakdown tests are performed in oil to increase the flashover voltage.

The choice of oil proved to be a significant challenge due to the extremely high field enhancement. Transformer oil (Nynas, $E_{bd} \approx 20$ kV/mm) provided enough dielectric strength to prevent flashover, but suffered from discharges at the electrode–insulation–oil triple point. This led to extreme degradation and puncturing of the insulation some distance from the electrode, which was deemed unrepresentative of the actual use case.

Choosing an oil with a higher breakdown strength showed a corresponding increase in the breakdown voltages which could be recorded. Silicone oil ($E_{bd} \approx 30$ kV/mm) provided a corresponding 1.5× increase in the audible PD inception voltage.

D. Results for Frequency and Waveform

First, ramp tests are performed for 50-Hz ac voltage and 25-, 50-, and 100-kHz square-wave and sinusoidal voltage. The Weibull distribution parameters for the 50-µm dielectric are summarized in Table I. The breakdown voltage (η parameter) shows a large dependence on frequency for the sine-wave voltage, but not for the square-wave voltage. This phenomenon is discussed in Section VII. The number of samples for each test was between 10 and 15 due to the low variance in the η parameter.

The trends in the data are visualized versus frequency and rise time in Fig. 6. The breakdown voltage under square-wave excitation is highly dependent on the rise time (i.e., its harmonic content) but not on the fundamental frequency in the range that is investigated (25–100 kHz).

TABLE I
RAMP TEST RESULTS FOR 50-µm DIELECTRIC

Test voltage	f	η [kV_{pk}]	β
Sinusoidal	50 Hz	8.6 ± 0.2	15.1
	25 kHz	7.8 ± 0.2	20.3
	50 kHz	7.4 ± 0.1	24.3
	100 kHz	7.0 ± 0.3	16.5
Square-wave ($t_r = 750$ ns)	25 kHz	6.4 ± 0.2	21.0
	50 kHz	6.5 ± 0.2	18.8
	100 kHz	6.3 ± 0.1	24.0

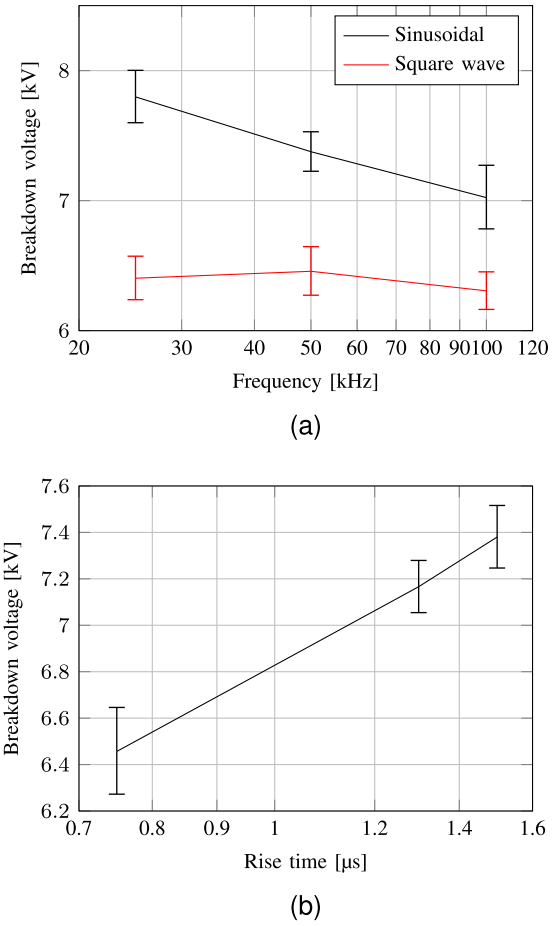

Fig. 6. Breakdown voltage of 50-µm dielectric versus (a) frequency and (b) rise time of square-wave voltage with $f = 50$ kHz.

E. Volume Effect and Thickness

Test results for a certain electrode diameter may be translated to a real PCB plane using the volume effect. Assuming that the test results are distributed according to a Weibull distribution with parameters η_1, β_1, a volume n times larger will have a distribution with

$$\eta_n = \eta_1 \cdot n^{-1/\beta_1} \quad (2)$$

$$\beta_n = \beta_1. \quad (3)$$

TABLE II
50-HZ AC BREAKDOWN VOLTAGES

t [µm]	η_{10} [kV]	η_{20} [kV]	η_{30} [kV]	β
50	6.0 ± 0.1	–	–	11.1
75	9.1 ± 0.3	8.0 ± 0.3	7.5 ± 0.5	10.7
100	11.8 ± 0.4	10.6 ± 0.4	10.1 ± 0.3	12.1

Note: no samples of 50 µm thickness were available with 20, 30 mm electrodes.

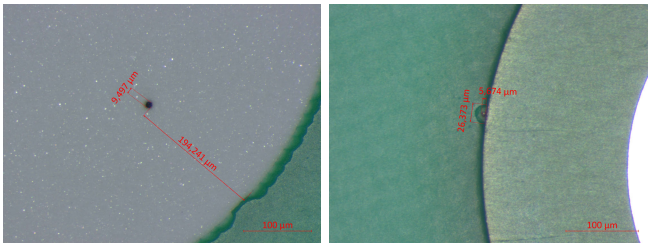

(a) (b)

Fig. 7. Micrographs of samples after breakdown. (a) At 50 Hz under the electrode; the copper was peeled off. (b) At 25 kHz at the electrode edge.

This effect is confirmed by performing ramp breakdown tests on three different electrode sizes (10-, 20-, and 30-mm diameter); see the β parameter in Table II. Between 15 and 25 samples were used for each thickness and electrode size combination.

As the dielectric thickness increases, the breakdown voltage is also expected to increase. The breakdown voltage is found to follow a power law versus thickness with exponent $k = 0.994 \pm 0.056$. Therefore, the breakdown voltage scales linearly with the dielectric thickness.

F. Breakdown Location

For these 50-Hz measurements, almost all the breakdown events occur at a random location under the electrode. However, when performing breakdown tests using HF sinusoidal voltage, most breakdowns were recorded at the edge of the electrode (see Fig. 7). This indicates a change in the breakdown mechanism at higher test frequencies.

V. LIFETIME TESTS

To determine the lifetime of the insulation under high-voltage stress, accelerated lifetime tests are performed at (constant) voltages above the nominal level. Weibull analysis is again performed on the obtained data, with the breakdown time t_{bd} as the random variable. Then, the lifetime L is estimated using an inverse power law regression model as follows:

$$L(U) = k\left(\frac{U}{U_0}\right)^{-n} \tag{4}$$

where k and n are the fitting parameters, U is the peak voltage, and U_0 is a normalizing constant set to 1 kV for this study. A log-voltage versus log-time plot results in a straight line with a slope of $(-1/n)$

$$\log L(U) = \log k - n \log(U/U_0). \tag{5}$$

TABLE III
LIFETIME RESULTS

t	f	n	L_0
50 µm	50 Hz	8.62 ± 4.48	22.7 ± 10.8
	25 kHz	9.61 ± 1.79	21.6 ± 3.1
	50 kHz	7.52 ± 1.19	17.8 ± 1.9
	100 kHz	9.82 ± 1.53	20.7 ± 2.4
75 µm	50 Hz	17.00 ± 6.11	45.0 ± 16.9
	25 kHz	9.48 ± 1.91	23.1 ± 3.6

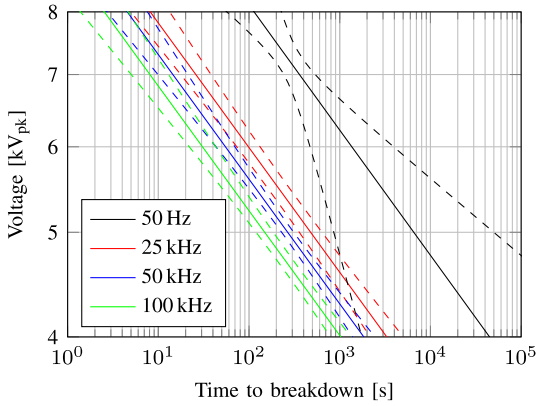

Fig. 8. Lifetime curves for 50-µm dielectric at 50 Hz compared with 25, 50, and 100 kHz. The high-frequency data are processed using the two assumptions: n is frequency-independent, and lifetime follows an inverse power law versus frequency.

The regression model is extended with the empirical relationship for the dependence on the fundamental frequency f

$$L(f) \propto \left(\frac{f}{f_0}\right)^{-\gamma} \tag{6}$$

from literature, where γ is usually around 1 for Type II materials and indicates the degree of high-frequency degradation.

A. Results

The extracted inverse power law parameters are presented in Table III. The slope of the life curve does not change appreciably over the tested frequency range, but the lifetime shows a decreasing trend. For the thicker insulation samples, there is a significant change in n from 50 Hz to 25 kHz. It is hypothesized that this is due to the change in breakdown mechanism mentioned in Section IV-F, but more tests are required.

Because of the statistical scatter in the measurement results, no conclusions can be drawn from the data in this representation. Therefore, two hypotheses from the literature are posed: 1) the slope n is constant versus frequency and 2) the lifetime is related to frequency by an inverse power law (6). The obtained data cannot reject these hypotheses and show that $\gamma = 0.84 \pm 0.25$, confirming the observations in literature for Type II materials [14]. Fig. 8 shows the voltage–life curves calculated using these assumptions. The slope $n = 8.56 \pm 0.87$. Type I materials (organic insulation) such as oil-impregnated paper show a much more severe dependence on frequency (i.e., $\gamma \gg 1$) above a certain critical field [20].

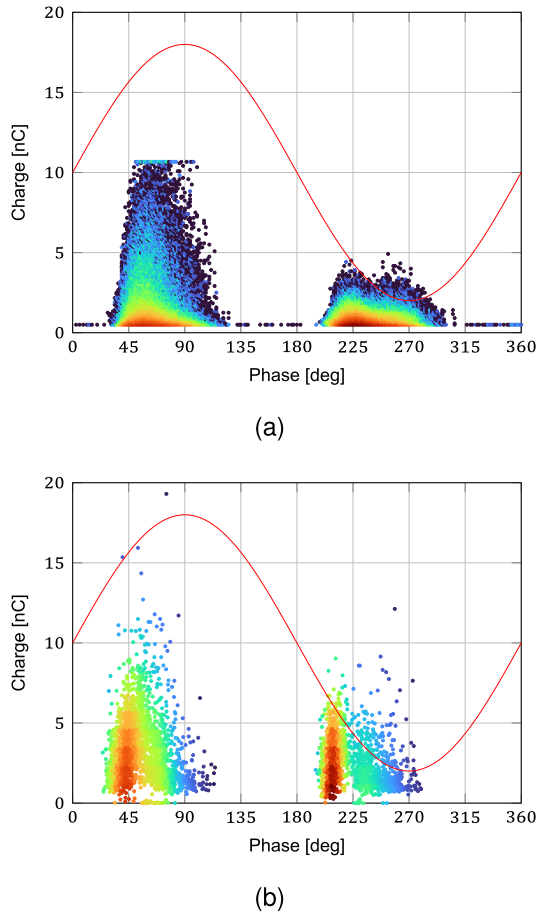

Fig. 9. PRPD of surface discharges under (a) 1.7 kV_{pk} at 50 Hz and (b) kV_{pk} at 25-kHz voltage stress on a sample with 50-μm dielectric. The color indicates the number of PD events per cycle.

VI. Degradation in Air

The preceding tests were performed under oil to study the properties of the dielectric. Under normal operating conditions, the PCBs are operated in air. Therefore, the degradation mechanisms that occur in air are investigated.

A. Partial Discharge

PDs on the surface of the IMS PCB ignite at voltages much lower than the breakdown voltage of the dielectric. This is due to the high fields that occur at the edge of the thin copper electrode. The PRPDs corresponding to surface discharges at 50 Hz and 25 kHz are presented in Fig. 9. The magnitude of the discharges is relatively large due to the capacitance of the sample. If discharges are ignited under high-frequency excitation, at least two discharges will occur per cycle, on the rising and falling voltage slope. This means that the repetition rate of PD is increased significantly compared with that measured with low-frequency voltage.

Further measurements of PD patterns and behavior over time are discussed in [1]. The main conclusions are that the PDIV is lower at high frequency, and that narrow cavity discharges and treeing appear to be the main sources of dielectric degradation in the material under study. PDs are only recorded for sinusoidal voltages, since the high dv/dt of the square-wave voltage interferes with the detection of PDs.

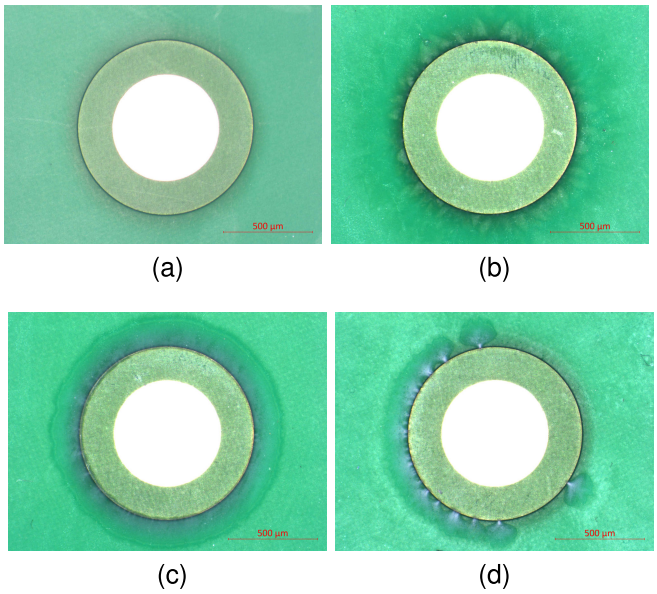

Fig. 10. Micrographs of surface degradation observed under various high-voltage stresses above the PDIV. (a) virgin sample, (b) 30 min at 50 Hz and 3 kV_{rms}, (c) 5 min at 25 kHz and 2.5 kV_{pk}, and (d) 5 min at 100 kHz and 2.5 kV_{pk}.

This can be resolved using the techniques presented by, e.g., Wang et al. [21].

B. Surface Degradation

When the sample is stressed above the surface discharge inception voltage, rapid degradation of the surface around the electrode is observed (e.g., Fig. 10). The growth of white trees is apparent already after 30 s of voltage application. This white powder has also been observed on FR4 PCBs with 50-Hz voltage after many hours of testing [4]. The powder can be wiped off the surface quite easily but leaves permanent damage to the solder mask. It is likely a byproduct of chemical degradation, since reactions with ozone result in chain scission and may generate peroxides, ketones, aldehydes, and carboxylic acids [22].

Observe that at higher frequency, the white tree-like structures are more concentrated and more severe than at low frequency, where the tree-like patterns are more diffuse. This can be explained with two observations from the PRPDs in Fig. 9: surface discharges at high frequency have: 1) a higher repetition rate and 2) a larger magnitude.

VII. Discussion

A. Short-Term Aging

Experiments have shown that the short-term breakdown voltage depends primarily on the rise time of the applied voltage waveform and not its fundamental frequency above 25 kHz, although these two parameters are related for sinusoidal waveforms. Dielectric heating is unlikely to be responsible for the observed phenomenon because the dielectric losses primarily depend on frequency and not rise time. Furthermore, the dielectric has a high thermal conductivity $\kappa_\theta = 3$ W/mK.

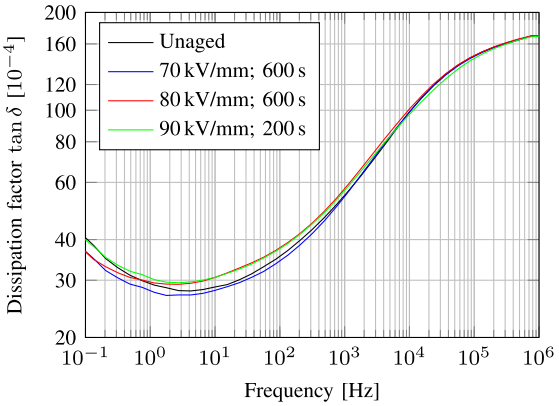

Fig. 11. Dielectric frequency response (tan δ) with aging under 25-kHz voltage stress. Measurement performed at 25 °C using Novocontrol Alpha dielectric spectrometer and Quatro Cryosystem.

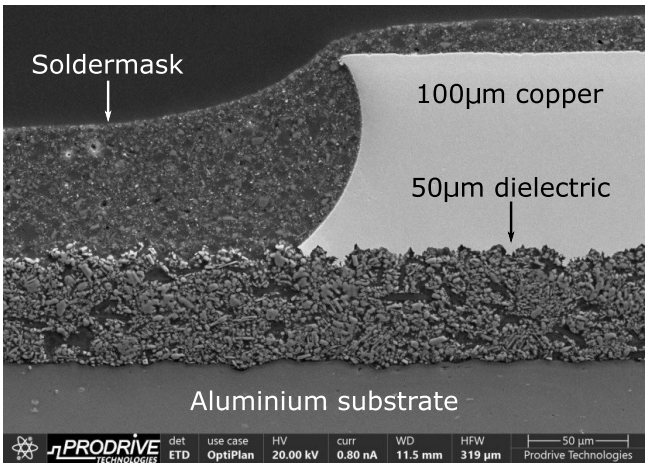

Fig. 12. SEM micrograph of the edge of a Cu plane. The PCB has 3-oz (100 µm) copper, 50-µm dielectric, and a 2-mm aluminum base. Image courtesy of Prodrive Technologies.

On the other hand, it has been shown that the PD magnitude is inversely proportional to the rise time [23], [24]. Given that at least one PD event will occur per period of the voltage waveform, PD erosion is a plausible short-term aging mechanism. For the thin samples under consideration, rapid PD erosion could lead to breakdown within a very short period of time. For the high-frequency tests, breakdown invariably occurred at the edge of the electrodes, whereas 50-Hz breakdown occurred underneath the electrodes. This also points to PD-driven degradation [25] or the rapid growth of electrical trees [26]. Nevertheless, the observed independence of the fundamental frequency cannot be explained this way. Further study with different frequencies and rise times is required to fully explain this phenomenon.

B. Long-Term Aging

The relationship between lifetime and frequency under sinusoidal voltage stress was found to be described by an inverse power law with $\gamma = 0.84 \pm 0.25$, i.e., almost inversely proportional. For the 50-µm insulation samples, the slope of the voltage–life curve was independent of the frequency of the voltage waveform. This agrees well with other experimental literature for Type II dielectrics.

Additional dielectric spectrum [dielectric frequency response (DFR)] measurements during the aging tests show no indication of a bulk change in either ε_r or $\tan\delta$; see Fig. 11. Therefore, it is hypothesized that the degradation is highly localized and does not affect the bulk dielectric properties. Such localized degradation could be related to the accelerated growth of trees under high-frequency electrical stress, which was also demonstrated in, e.g., [26].

C. Surface Degradation

Besides electrical breakdown through the sample, a dominant degradation factor was found to be due to discharges on the surface of the PCB, which is covered by the solder mask. Note that the patterns observed in Fig. 10 follow the same behavior as [26]: as the frequency increases, the branches of the surface trees become denser and then more concentrated.

As shown in Fig. 12, the etching process can leave very sharp edges on the copper planes, resulting in significant enhancement of the field which is already high due to the thin dielectric. If the solder mask is damaged or too thin (note the nonuniform thickness in the figure), PDs can easily occur at the corners. This risk can be mitigated by using a double solder mask or conformal coating on the edges of the planes.

VIII. Conclusion

This article investigated the dielectric aging and breakdown of IMS PCBs under 50 Hz and high-frequency voltage stresses. Short-term breakdown and long-term aging tests show that the dielectric layer itself is robust, with breakdown fields on the order of 120–160 kV/mm. The insulation lifetime is found to vary nearly inversely with frequency. Degradation of the solder mask and dielectric due to surface discharges occurs way before any internal aging mechanism, thus limiting the useable voltage–lifetime. Such degradation is severely enhanced under high-frequency voltage stress and can lead to tree formation within minutes after discharge inception.

Acknowledgment

The authors express their appreciation to the High Voltage Technology Group of Delft University of Technology and Prodrive Technologies for the material support.

References

[1] G. Lagerweij, "Reliability and ageing of IMS PCBs in high-voltage power electronic applications," Master's thesis, Dept. High Voltage Technol. group, Elect. Sustain. Energy, Delft University of Technology, Delft, The Netherlands, 2023.

[2] B. Du, "Temperature dependence of surface breakdown on printed circuit board," in *Proc. Electr. Insul. Conf. Electr. Manuf. Coil Winding Technol. Conf.*, Sep. 2003, pp. 167–170.

[3] B. Du, Y. Liu, and H. Liu, "Effects of low pressure on tracking failure of printed circuit boards," *IEEE Trans. Dielectr. Electr. Insul.*, vol. 15, no. 5, pp. 1379–1384, Oct. 2008.

[4] C. Emersic, C. Zhang, I. Cotton, R. Lowndes, S. Rowland, and R. Freer, "Degradation of printed circuit board coatings due to partial discharge," in *Proc. IEEE Electr. Insul. Conf. (EIC)*, Jun. 2015, pp. 420–423.

[5] C. Emersic, R. Lowndes, I. Cotton, S. Rowland, and R. Freer, "Observations of breakdown through printed circuit board polymer coatings via a surface pollution layer," *IEEE Trans. Dielectr. Electr. Insul.*, vol. 24, no. 4, pp. 2570–2578, Apr. 2017.

[6] Q. Zhou et al., "Study on insulation breakdown characteristics of printed circuit board under continuous square impulse voltage," *Energies*, vol. 11, no. 11, p. 2908, Oct. 2018.

[7] K. Monden, "Equivalent thermal conductivity of insulating layer in insulated metal substrates," *Adv. Sci. Tech.*, vol. 45, pp. 2664–2669, Aug. 2006.
[8] S. Kim, J. Kim, and J. Hyeok Kim, "Fabrication of insulated metal substrates with organic ceramic composite films for high thermal conductivity," *Ceram. Int.*, vol. 43, no. 11, pp. 8294–8299, Aug. 2017.
[9] Z. Li, K. Okamoto, Y. Ohki, and T. Tanaka, "Effects of nano-filler addition on partial discharge resistance and dielectric breakdown strength of micro-Al_2O_3Epoxy composite," *IEEE Trans. Dielectr. Electr. Insul.*, vol. 17, no. 3, pp. 653–661, Jun. 2010.
[10] J. Dong et al., "Effect of temperature gradient on space charge behavior in epoxy resin and its nanocomposites," *IEEE Trans. Dielectr. Electr. Insul.*, vol. 24, no. 3, pp. 1537–1546, Jun. 2017.
[11] D. Fabiani, G. C. Montanari, A. Krivda, L. E. Schmidt, and R. Hollertz, "Epoxy based materials containing micro and nano sized fillers for improved electrical characteristics," in *Proc. 10th IEEE Int. Conf. Solid Dielectr.*, Jul. 2010, pp. 1–4.
[12] M. Ghassemi, "Accelerated insulation aging due to fast, repetitive voltages: A review identifying challenges and future research needs," *IEEE Trans. Dielectr. Electr. Insul.*, vol. 26, no. 5, pp. 1558–1568, Oct. 2019.
[13] P. Mathew and M. G. Niasar, "Lifetime of oil-impregnated paper under pulse stress at different frequencies," in *Proc. Nordic Insul. Symp.*, Jul. 2022, vol. 27, no. 1. [Online]. Available: https://www.ntnu.no/ojs/index.php/nordis/article/view/4713
[14] A. Cavallini, D. Fabiani, and G. C. Montanari, "Power electronics and electrical insulation systems–part 2: Life modeling for insulation design," *IEEE Elect. Insul. Mag.*, vol. 26, no. 4, pp. 33–39, Jul. 2010.
[15] Y. Zang et al., "Optical detection method for partial discharge of printed circuit boards in electrified aircraft under various pressures and voltages," *IEEE Trans. Transport. Electrific.*, vol. 8, no. 4, pp. 4668–4677, Dec. 2022.
[16] S. Yu, W. Wang, Q. Jiang, L. Hu, and J. He, "Breakdown characteristics of epoxy dielectric film under high frequency square wave voltage," in *Proc. IEEE 4th Int. Conf. Dielectr. (ICD)*, Jul. 2022, pp. 680–683.
[17] G. Lagerweij and M. G. Niasar, "Design of a high-frequency transformer based on amorphous cut cores for insulation breakdown testing," *High Voltage*, vol. 9, no. 5, pp. 1183–1194, Oct. 2024.
[18] W. Zhao, G. W. Lagerweij, and M. G. Niasar, "Design of a high-voltage high-frequency insulation test system using a ferrite-based resonant transformer," *High Volt.*, Sep. 2024.
[19] M. Ghaffarian Niasar, "Mechanisms of electrical ageing of oil-impregnated paper due to partial discharges," Ph.D. dissertation, Division Electromagn. Eng., KTH School of Electrical Engineering, Stockholm, Sweden, Feb. 2015.
[20] P. Mathew, M. G. Niasar, and P. Vaessen, "Design of high-frequency fast-rise pulse modulators for lifetime testing of dielectrics," *IEEE Trans. Dielectr. Electr. Insul.*, vol. 30, no. 6, pp. 2798–2808, Dec. 2023.
[21] Z. Wang et al., "Partial discharge behavior of high frequency transformer insulation under high voltage PWM stress," *IEEE Trans. Dielectr. Electr. Insul.*, 2025.
[22] N. Dehlinger and G. Stone, "Surface partial discharge in hydrogenerator stator windings: Causes, symptoms, and remedies," *IEEE Elect. Insul. Mag.*, vol. 36, no. 3, pp. 7–18, 2020.
[23] P. Wang, A. Cavallini, G. C. Montanari, and G. Wu, "Effect of rise time on PD pulse features under repetitive square wave voltages," *IEEE Trans. Dielectr. Electr. Insul.*, vol. 20, no. 1, pp. 245–254, Feb. 2013.
[24] P. Wang, A. Cavallini, and G. C. Montanari, "The influence of repetitive square wave voltage parameters on enameled wire endurance," *IEEE Trans. Dielectr. Electr. Insul.*, vol. 21, no. 3, pp. 1276–1284, Jun. 2014.
[25] F. Küchler, R. Färber, F. Bill, S. Renggli, and C. M. Franck, "Mixed-frequency medium-voltage aging analysis of epoxy in the absence of partial discharges and dielectric heating," *J. Phys. D, Appl. Phys.*, vol. 56, no. 35, Aug. 2023, Art. no. 355502.
[26] Y. Zhang, Y. Zhou, X. Zhu, C. Teng, T. Zhang, and D. Hu, "Electrical tree evolution of BN sheet/epoxy resin composites at high voltage frequencies," *IEEE Trans. Dielectr. Electr. Insul.*, vol. 29, no. 5, pp. 1991–1999, Oct. 2022.

Gijs Willem Lagerweij was born in Dordrecht, The Netherlands, in 2000. He received the B.Sc. degree (cum laude) in electrical engineering and the M.Sc. degree (cum laude) in electrical power engineering from Delft University of Technology (TU Delft), Delft, The Netherlands, in 2021 and 2023, respectively.

He joined Prodrive Technologies, Eindhoven, The Netherlands, in 2020, as a Power Electronics Engineer and is currently working there as the Global Competence Owner for magnetic component design. His main research interests are high-precision power electronics, magnetic components, and insulation systems for power electronics.

Mohamad Ghaffarian Niasar (Member, IEEE) was born in Tehran, Iran, in 1984. He received the M.Sc. degree from the Sharif University of Technology, Tehran, in 2008, and the Ph.D. degree in electrical engineering from the Royal Institute of Technology (KTH), Stockholm, Sweden, in 2015.

He is currently an Associate Professor with the High Voltage Technologies Group, Delft University of Technology, Eindhoven, The Netherlands. His main research interests are aging of electrical insulation, high-voltage power electronics, HVdc insulation systems, partial discharges, high-frequency power transformers, power cables, and multiphysics FEM modeling.